Title

Analysis of Concordance Between Next-Generation Sequencing Assessment of Microsatellite Instability and Immunohistochemistry-Mismatch Repair From Solid Tumors.

Permalink

Authors

Ali-Fehmi, Rouba

Krause, Harris

Morris, Robert

et al.

Publication Date

DOI

Analysis of Concordance Between Next-Generation Sequencing Assessment of Microsatellite Instability and Immunohistochemistry-Mismatch Repair From Solid Tumors

Rouba Ali-Fehmi, MD[1]; Harris Benjamin Krause, PhD[2]; Robert T. Morris, MD[3,4]; John J. Wallbillich, MD[3,4]; Logan Corey, MD[3,4]; Sudeshna Bandyopadhyay, MD[3,4]; Mira Kheil, MD[3,4]; Leana Elbashir, MD[3,4]; Fadi Zaiem, MD[3,4]; M. Ruhul Quddus, MD[5]; Evi Abada, MD, MS[3,5]; Thomas Herzog, MD[6]; Anthony N. Karnezis, MD, PhD[7]; Emmanuel S. Antonarakis, MD[8]; Pashtoon Murtaza Kasi, MD, MS[9]; Shuanzeng Wei, MD, PhD[10]; Jeffrey Swensen, PhD[2]; Andrew Elliott, PhD[2]; Joanne Xiu, PhD[2]; Jaclyn Hechtman, MD[2]; David Spetzler, MS, PhD, MBA[2]; Jim Abraham, PhD[2]; Milan Radovich, PhD[2]; George Sledge, MD[2]; Matthew J. Oberley, MD, PhD[2]; and David Bryant, MD, PhD[2]

ABSTRACT

PURPOSE The new CAP guideline published in August 2022 recommends using immunohistochemistry (IHC) to test for mismatch repair defects in gastroesophageal (GE), small bowel (SB), or endometrial carcinoma (EC) cancers over next-generation sequencing assessment of microsatellite instability (NGS-MSI) for immune checkpoint inhibitor (ICI) therapy eligibility and states there is a preference to use IHC over NGS-MSI in colorectal carcinoma (CRC).

METHODS We assessed the concordance of NGS-MSI and IHC-MMR from a very large cohort across the spectrum of solid tumors.

RESULTS Of the over 190,000 samples with both NGS-MSI and IHC-MMR about 1,160 were initially flagged as discordant. Of those samples initially flagged as discordant, 50.9% remained discordant after being reviewed by an additional pathologist. This resulted in a final discordance rate of 0.31% (590/191,767). Among CRC, GE, SB and EC, 55.4% of mismatch repair proficient/MSI high (MMRp/MSI-H) tumors had at least one somatic pathogenic mutation in an MMR gene or *POLE*. Mismatch repair deficient/microsatellite stable (MMRd/MSS) tumors had a significantly lower rate of high tumor mutational burden than MMRp/MSI-H tumors. Across all solid tumors, MMRd/MSI-H tumors had significantly longer overall survival (OS; hazard ratio [HR], 1.47, *P* < .001) and post-ICI survival (HR, 1.82, *P* < .001) as compared with MMRp/MSS tumors. The OS for the MMRd/MSS group was slightly worse compared to the MMRp/MSI-H tumors, but this difference was not statistically significant (HR, 0.73, *P* = .058), with a similar pattern when looking at post-ICI survival (HR, 0.43, *P* = .155).

CONCLUSION This study demonstrates that NGS-MSI is noninferior to IHC-MMR and can identify MSI-H tumors that IHC-MMR is unable to detect and conversely IHC-MMR can identify MMRd tumors that NGS-MSI misses.

INTRODUCTION

MLH1/PMS2 and MSH2/MSH6 are proteins that form heterodimers and play a critical role and in the recognition and initiation of DNA mismatch repair (MMR).[1] Expression of the MMR proteins can be assessed directly via immunohistochemistry (IHC) and categorized as MMR proficient (MMRp) or MMR deficient (MMRd). Microsatellite instability (MSI) status can also be assessed via polymerase chain reaction (PCR) or next-generation sequencing (NGS)[3,4] and categorized as MSI high (MSI-H) or microsatellite stable (MSS). PCR-MSI or NGS-MSI is highly correlated with IHC-defined MMR status (IHC-MMR).[5-9] MMRd/MSI-H tumors can benefit from treatment with immune checkpoint inhibitors (ICIs).[10] An advantage of using NGS-MSI is that many patients are already undergoing NGS to identify somatic mutations that could inform the treatment they receive; assaying for MSI status at the same time reduces tissue consumption although IHC may have a faster turnaround time and be more likely to succeed when there is low neoplastic content.

CAP guidelines published in August 2022[11] proposed IHC testing for MMR defects or testing for MSI status via PCR or

CONTEXT

Key Objective
What is the concordance between next-generation sequencing assessment of microsatellite instability (NGS-MSI) and immunohistochemistry (IHC) for mismatch repair defects across different solid tumors, in accordance with the 2022 CAP guideline recommendations.

Knowledge Generated
A discordance rate of only 0.31% was noted between NGS-MSI and IHC-MMR. Additionally, NGS-MSI proves to be non-inferior to IHC-MMR for mismatch repair defects assessment.

Relevance
This study demonstrated high concordance between NGS-MSI and IHC-MMR, and no difference in overall survival between discordant tumors was observed. NGS-MSI can detect mismatch repair deficiencies that IHC-MMR does not detect, and conversely IHC-MMR can detect some mismatch repair deficiencies that NGS-MSI cannot; thus, no one technology captures all cases of mismatch repair deficiency. Based on the reported rates of discordance, for every 1,111 patient tested with NGS-MSI, one patient will be identified as microsatellite instability high (MSI-H) that MMR-IHC would not have identified.

IHC-MMR in gastroesophageal (GE), small bowel (SB), or endometrial carcinoma (EC) tumors over NGS of MSI (NGS-MSI) for ICI therapy eligibility. For colorectal carcinoma (CRC), PCR and IHC-MMR were preferred over NGS-MSI. These recommendations suggest that IHC generally is preferable to NGS-MSI to evaluate ICI therapy recommendations because of reduced cost of the assay and lack of published evidence of concordance with IHC-MMR. In the guidelines, two studies that had previously investigated the concordance between IHC-MMR and NGS-MSI were cited as evidence of the concordance of IHC-MMR and NGS-MSI testing. These studies were limited by their sample sizes (n = 91, CRC[12] and n = 12,288, pan-tumor[13]). Hechtman et al[14] investigated 443 tumors with IHC-MMR and NGS-MSI-H results and found that MMRp/MSI-H discordant tumors had an enrichment of missense over truncating mutations in MMR proteins. However, the results were limited by their sample, and clinical outcomes were reported for only three patients.

We assessed the concordance of NGS-MSI versus IHC-MMR from a cohort of 190,000 tumors across a large spectrum of cancer types and studied the molecular characteristics, immunological landscape, and clinical outcome of these patients.

METHODS

Next-Generation Sequencing-592 Gene Panel/Whole-Exome Sequencing

NGS-592 or whole-exome sequencing (WES) was performed for 191,767 solid tumors (CRC: n = 28,105, GE: n = 9,849, SB: n = 1,405, EC: n = 14,129) sequenced at Caris Life Sciences (Appendix 1).

Identification of Genetic Variants

Genetic somatic variants identified were interpreted by board-certified molecular geneticists and categorized as pathogenic, likely pathogenic, variant of unknown significance, likely benign, or benign (Appendix 2).

MSI Status by NGS-592/WES

The details of this MSI analysis for NGS-592 have been described previously.[15] Details on MSI by WES can be found in Appendix 3.

Whole-Transcriptome Sequencing

Whole-transcriptome sequencing was conducting on micro dissected tumor content and sequenced using the Illumina NovaSeq platform (Illumina, Inc, San Diego, CA; Appendix 4).

Mismatch Repair Protein Expression by IHC

IHC was performed on formalin-fixed paraffin-embedded sections on glass slides. Slides were stained using automated staining techniques, per the manufacturer's instructions, and were optimized and validated per Clinical Laboratory Improvement Amendments/CAP and ISO requirements. Board-certified pathologists evaluated all IHC results independently.

MMR protein expression was tested by IHC using antibody clones (MLH1, M1 antibody; MSH2, G2191129 antibody; MSH6, 44 antibody; and PMS2, EPR3947 antibody [Ventana Medical Systems, Inc, Tucson, AZ]). The complete absence of

protein expression for any of the four proteins tested was considered MMRd and MMRp as positive staining in all four proteins.

Tumor Mutational Burden

For the NGS-592 and WES assays, tumor mutational burden (TMB) was measured by counting all nonsynonymous missense, nonsense, inframe insertion/deletion, and frameshift mutations found per tumor that had not been previously described as germline alterations in dbSNP151, Genome Aggregation Database, or benign variants identified by Caris geneticists. A cutoff point of ≥10 mutations per Mb (mut/Mb) was used based on the KEYNOTE-158 pembrolizumab trial,[16] which showed that patients with a TMB of ≥10 mt/MB (TMB-H) across several tumor types had higher response rates than patients with a TMB of <10 mt/MB.[17] Caris was a member of the friends of cancer consortium and are aligned with their standards.[18]

Discordant Cases and Pathology Review

Cases where MMR and MSI calls were discordant are triggered for review by an additional pathologist who reevaluates the IHC staining. For this study, to further confirm that the MMR IHC determination on discordant cases after this initial reevaluation are correct, CRC (n = 74), GE (n = 31), SB (n = 7), and EC (n = 90) with discordant MMR/MSI results that had digitized slides available were re-reviewed (central pathology review [CPR]) by two senior board-certified pathologists (R.A.-F., D.B.). Each pathologist re-reviewed all slides digitally independently and were blinded to each other's interpretations. When a disagreement arose during CPR, a consensus interpretation was obtained by re-evaluating and discussing the case together. NGS-MSI results were not reviewed on these discordant cases as the MSI result is derived from an algorithm and is not subjectively interpreted like MMR-IHCs are. We acknowledge that NGS-MSI can have lower performance and may produce false MSI-stable results at lower percentages of tumor nuclei. Our laboratory-developed assay has been appropriately validated down to our minimum input of 20% tumor nuclei, but this could be a limitation of our study.

Clinical Outcomes

Real-world overall survival was obtained from insurance claims and calculated from either tissue collection or from start of ICIs (atezolizumab, avelumab, nivolumab, or pembrolizumab) to last contact. Kaplan-Meier estimates were calculated for molecularly defined patients. Cohorts used were MMRd/MSI-H versus MMRp/MSS and MMRd/MSS versus MMRp/MSI-H tumors. These cohorts were applied to all available tumors in addition to CRC, GE/SB, and EC tumors.

Statistical Methods

Descriptive analyses were conducted using Mann-Whitney U (scipy V.1.9.3) and X^2/Fisher exact tests (R v.3.6.1) for continuous and categorical variables, respectively. P values were adjusted for multiple comparisons, with $q < 0.05$ considered significant when appropriate. All listed HRs use the Cox proportional hazards model, and the P values were calculated using the log-rank statistic.[19]

Ethics Approval and Consent to Participate

This study was conducted in accordance with the guidelines of the Declaration of Helsinki, Belmont Report, and US Common Rule. In keeping with 45 CFR 46.101 (b), this study was performed using retrospective, deidentified clinical data. Therefore, this study was deemed Institutional Review Board exempt, and no patient consent was necessary from the patients.

RESULTS

Concordance Across All MSI and MMR Tested Cases

All tumors (N = 191,767) that received IHC staining for MMR protein and had MSI data available were investigated. Discordant tumors (MSI and MMR in disagreement) were re-reviewed by board-certified pathologists; 50.80% of the cases flagged as discordant became concordant after they were reviewed again by a pathologist (this process was independent of the CPR that was conducted for this paper), and 99.60% of tumors (191,177/191,767) were concordant; 0.31% (590/191,767) of tumors remained discordant after being re-reviewed. For the discordant tumors, 30.8% (182/590) were MMRp/MSI-H and 69.2% (408/590) were MMRd/MSS; the level of discordance was evenly distributed across the solid tumors that were investigated (Table 1). Of note, in 0.76% of tested samples, both NGS-MSI and IHC-MMR results were indeterminate, and in 7.9% of samples, NGS-MSI was indeterminate and IHC-MMR was successful, and in 2.6% of samples, NGS-MSI was successfully run and IHC-MMR was indeterminate.

Pathology Review of a Subset of Discordant Cases

Of the 590 discordant cases, the four histologies with the highest rate of mismatch repair deficiency (CRC, GE, SB, and EC) were chosen for review, which consisted of 210 cases. Of these 210 discordant cases, 202 were available to be taken out of long-term storage and digitized. These 202 cases then underwent CPR to confirm the MMR diagnosis. 94% (46/49) of CRC that were MMRp/MSI-H were confirmed to be MMRp after review. However, the percent of diagnosis confirmed was much lower for GE (44%, 4/9), (75% 3/4), and EC (71%, 30/42) tumors (Table 2). Of the 202 reviewed discordant cases, 21 tumors were reclassified from MMRp to MMRd during pathology review. Of these, 66.7% (14/21) had loss of PMS2 and 47.6% (10/21) had loss of MLH1 (Fig 1).

Of the tumors that were initially classified as MMRd/MSS, 95.9% (94/98) were confirmed to be MMRd after review, and all four tumor types investigated had agreement rates of >95% (Table 2). After pathology review, the percentage

TABLE 1. Concordance and Discordance of NGS-MSI Versus IHC-MMR From a Cohort of 190,000 Tumors Across a Large Spectrum of Cancer Types

Cancer Type	Concordant MMRd/MSI-H	Discordant MMRd/MSS	Concordant MMRp/MSS	Discordant MMRp/MSI-H	% Concordance
All	6,913	408	184,264	182	99.69
CRC	1,884	25	26,147	49	99.74
GE	480	22	9,338	9	99.69
SB	124	3	1,274	4	99.50
EC	2,740	48	11,299	42	99.36
Others	1,685	310	136,206	78	99.72

Abbreviations: CRC, colorectal carcinoma; EC, endometrial carcinoma; GE, gastroesophageal; MMRd, mismatch repair deficient; MMRp, mismatch repair proficient; MSI-H, microsatellite instability high; MSS, microsatellite stable; NGS-MSI, next-generation sequencing assessment of microsatellite instability; SB, small bowel.

discordance decreased further across all investigated tumor types (Table 2).

Discordant MMRp/MSI–H Tumors

We next investigated pathogenic/likely pathogenic variants (PLP variants) that could be responsible for the observed MMRp/MSI–H discordance. Missense PLP variants *MLH1*, *MSH2*, *MSH6*, or *PMS2* were classified as Group 1. Any PLP variants to alternative MMR genes (*MLH3*, *MSH3*, *PMS1*) were classified as Group 2, and PLP variants in *POLE* are classified as Group 3.

In total, 55.4% (46/83) of MMRp/MSI–H tumors had at least one Group 1, 2, or 3 PLP variants, and 28.9% (24/83) tumors had at least one Group 1 mutation. Of group 1, 95.8% (23/24) had just one group 1 variant present: 45.6% (11/24) had a *MLH1*

variant, 20.8% (5/24) had a *MSH2* variant, 33.3% (8/24) had an *MSH6* variant, and 4.2% (1/24) had a *PMS2* variant. The tumor that had two simultaneous group 1 PLP variants was a uterine neoplasm that had mutations in *PMS2* and *MSH6* (affecting both MMR heterodimers). Of samples that had a Group 2 mutation, 87.5% (14/16) had a mutation in *MSH3*. Finally, 18.1% (15/83) of tumors had a *POLE* mutation. Of these tumors, 93.3% (14/15) had no other Group 1 or 2 mutations (Fig 2).

Another possible reason for MMRp/MSI–H discordance is that there is clonal loss (heterogeneous staining) of one of the stained for MMR proteins. Of all MMRp/MSI–H samples that were confirmed by pathology review, 9.6% (8/83) had clonal loss of at least one MMR protein. Of the eight tumors that had clonal loss of at least one MMR protein, 83.3% (6/8) had clonal loss of both MLH1 and PMS2, all of them EC tumors.

TABLE 2. Concordance/Discordance of NGS-MSI and IHC-MMR After CPR for CRC, GE, SB, and EC Tumors

Subgroup	No. of Samples with IHC and MSI Data	No. of MMRp/MSI-H Samples Undergoing Pathology Review	MMRp After Pathology Review	% Discrepant Cases Resolved	Percent Discordant Postreview
CRC MMRp/MSI-H	30,835	49	46	6	0.15
GE MMRp/MSI-H	10,743	9	4	56	0.04
SB MMRp/MSI-H	1,528	4	3	25	0.20
EC MMRp/MSI-H	15,150	42	30	29	0.20
Combined MMRp/MSI-H	58,256	104	83	20	0.14

Subgroup	No. of Samples With IHC and MSI Data	No. of MMRd/MSS Samples Undergoing Pathology Review	MMRd After Pathology Review	% Discrepant Cases Resolved	Percent Discordant Postreview
CRC MMRd/MSS	30,835	25	24	4	0.08
GE MMRd/MSS	10,743	22	21	5	0.20
SB MMRd/MSS	1,528	3	3	0	0.20
EC MMRd/MSS	15,150	48	46	4	0.30
Combined MMRd/MSS	58,256	98	94	4	0.16

Abbreviations: CPR, central pathology review; CRC, colorectal carcinoma; EC, endometrial carcinoma; GE, gastroesophageal; IHC, immunohistochemistry; MMRd, mismatch repair deficient; MMRp, mismatch repair proficient; MSI-H, microsatellite instability high; MSS, microsatellite stable; NGS-MSI, next-generation sequencing assessment of microsatellite instability; SB, small bowel.
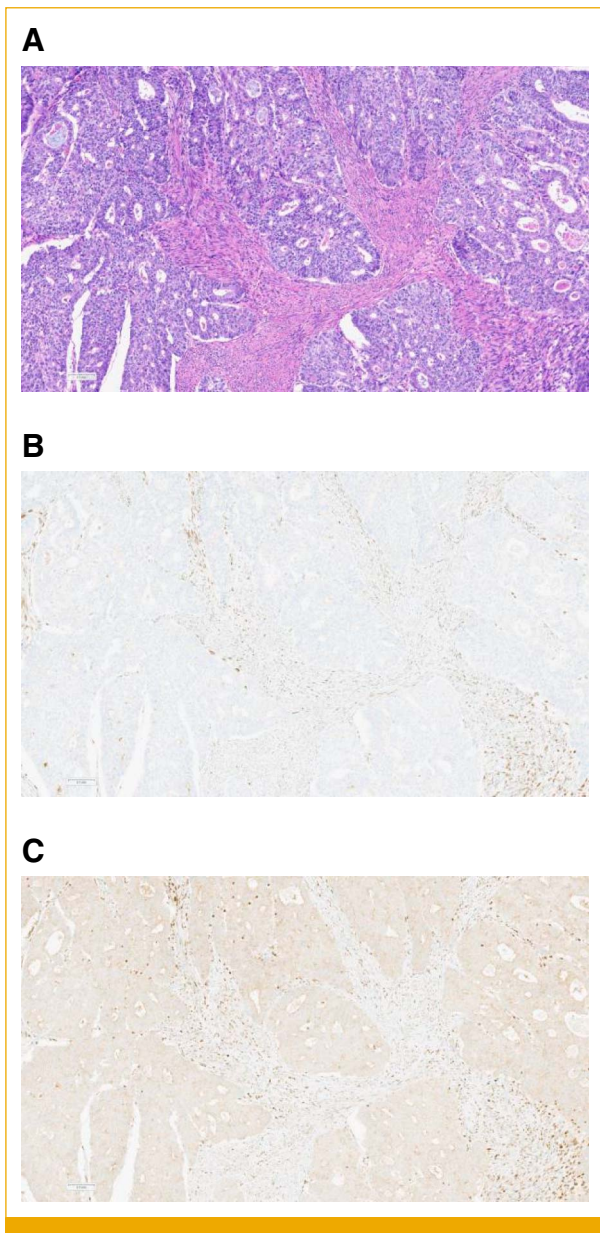
FIG 1. (A) H&E, (B) MLH1, and (C) PMS2 at 10× magnification showing an EC tumor with loss of nuclear expression for MLH1 and PMS2. This tumor was MMRd/MSI-H. EC, endometrial carcinoma; H&E, hematoxylin and eosin; MMRd, mismatch repair deficient; MSI-H, microsatellite instability.

Discordant MMRd/MSS Tumors

Of the 94 post–CPR MMRd/MSS tumors, 32% (30/94) had MLH1 loss, 70% (65/94) PMS2 loss, 3% (3/94) MSH2 loss, and 31% (29/94) MSH6 loss (by IHC; denominator represents tumors that had slides available for that stain; Appendix 5).

In specific MSI assays, MSH6 can show a loss of protein but atypical mutational spectra that does not confer MSI-H phenotype.[20-22] Among MMRd/MSS tumors, 2 of 24 CRC, 3 of 21 GE, 1 of 3 SB, and 19 of 46 EC tumors had an isolated loss of

MSH6. Among MMRd/MSS tumors, 2 of 21 GE and 2 of 46 EC tumors had nonisolated loss of MSH6, and no MSH6 mutations were observed in the nonisolated loss group. Unique mutations were observed in the isolated loss group (sometime multiple per tumor, variants of unknown significance are included), but almost no recurrent mutations were identified.

Previous work[23] has shown that nonpathogenic mutations in *MLH1* can be responsible for discordance between NGS-MSI and IHC-MMR. Of the tumors that underwent pathology review, 12% (3/25) of MMRd/MSS tumors with MLH1 loss had nonpathogenic mutations in *MLH1* including E717D, L296S, and M242V.

TMB and the Tumor Immune Microenvironment of Discordant Cases

When concordant tumors were investigated, MMRd/MSS CRC, EG/SB and EC tumors had a significantly lower rate of TMB-H than MMRp/MSI-H tumors (Fig 3A). The prevalence of TMB-H in CRC discordant tumors was compared with concordant tumors. The magnitude of difference was the largest between MSS versus MSI-H tumors regardless of MMR status. MMRd/MSI-H had a significantly higher TMB-H prevalence than MMRp/MSS, and MMRp/MSI-H had a significantly lower TMB-H prevalence as compared with MMRd/MSI-H (Fig 3B). Similar results are observed for TMB-H prevalence in GE/SB and EC tumors (Appendix 6).

Using immune deconvolution of bulk RNA-seq data (QuanTIseq), we investigated the immune microenvironment across CRC, EC, and GE/SB tumors. The EC cohort is a mixture of histologic subtypes, endometrioid, serous, clear cell, and carcinosarcoma among others and was not separately analyzed by specific histology. Our patient population is also enriched with higher staged disease than the typical practice. No significant difference in immune infiltrate was observed between the MMRd/MSS and MMRp/MSI-H cohort ($q > 0.05$). However, MMRp/MSI-H CRC tumors had 4% more M1 macrophage infiltrate as compared with MMRd/MSS CRC tumors ($P < .05$; Fig 3C).

Survival Outcomes on the Basis of Discordance

When comparing clinical outcomes of concordant tumors across all investigated solid tumors, concordant MMRd/MSI-H patients had significantly longer OS (HR, 1.472 [95% CI, 1.408 to 1.538]; $P < .001$, Fig 4A) as did post-ICI survival (HR, 1.818 [95% CI, 1.627 to 2.032]; $P < .001$, Fig 4B). Compared with MMRp/MSI-H tumors, MMRd/MSS had similar OS that was trending worse for the MMRd/MSS cohort (HR, 0.728 [95% CI, 0.523 to 1.013]; $P = .058$, Fig 4C), with a similar pattern when looking at post-immunotherapy (IO) survival (HR, 0.429 [95% CI, 0.129 to 1.429]; $P = .155$, Fig 4D). A similar pattern is observed when comparing concordant and discordant tumors in cancer-specific contexts (CRC, GE/SB, and EC).

Cancer type			CRC	GE/SB	EC
Group 1 mutation	MLH1	Missense			
	MSH2	Missense			
	MSH6	Missense			
	PMS2	Missense			
Group 2 mutation	MLH3	Mutant			
	MSH3	Mutant			
	PMS1	Mutant			
Group 3 mutation	POLE	Mutant			

Positive ☐ Negative

FIG 2. Oncoprint of MMRp/MSI-H tumors with at least one of the eight investigated mutations. For Group 1 mutations, positive indicates a pathogenic missense mutation and negative indicated no pathogenic missense mutation. For Group 2 and POLE Mutant, positive indicates any pathogenic mutation and negative indicates no pathogenic mutations. CRC, colorectal carcinoma; EC, endometrial carcinoma; GE, gastro-esophageal; MMRp, mismatch repair proficient; MSI-H, microsatellite instability high; SB, small bowel.

DISCUSSION

MSI can be caused by germline mutations (Lynch syndrome) or somatic alterations (mutations, *MLH1* promoter methylation) of DNA–mismatch repair enzymes including *MSH2*, *MSH6*, *PMS2*, and *MLH1*.[24,25] For patients with Lynch syndrome, MSI occurs in non–neoplastic in addition to cancerous cells.[26] Among GI tract malignancies, dMMR/MSI–H

FIG 3. (A) TMB-H prevalence for the four investigated tumor types. (B) Prevalence of TMB-H for discordant and concordant CRC tumors ($q < 0.05$ as indicated by asterisk for both). (C) Difference in immune cell infiltrate between MSS/MMRd and MSI-H/MMRp tumors in three cancer groups ($P < .05$ denoted by black asterisk, $q > 0.05$ for all immune cell population comparisons). CRC, colorectal carcinoma; EC, endometrial carcinoma; GE, gastroesophageal; MMRd, mismatch repair deficient; MMRp, mismatch repair proficient; MSS, microsatellite stable; MSI-H, microsatellite instability high; SB, small bowel; TMB, tumor mutational burden.
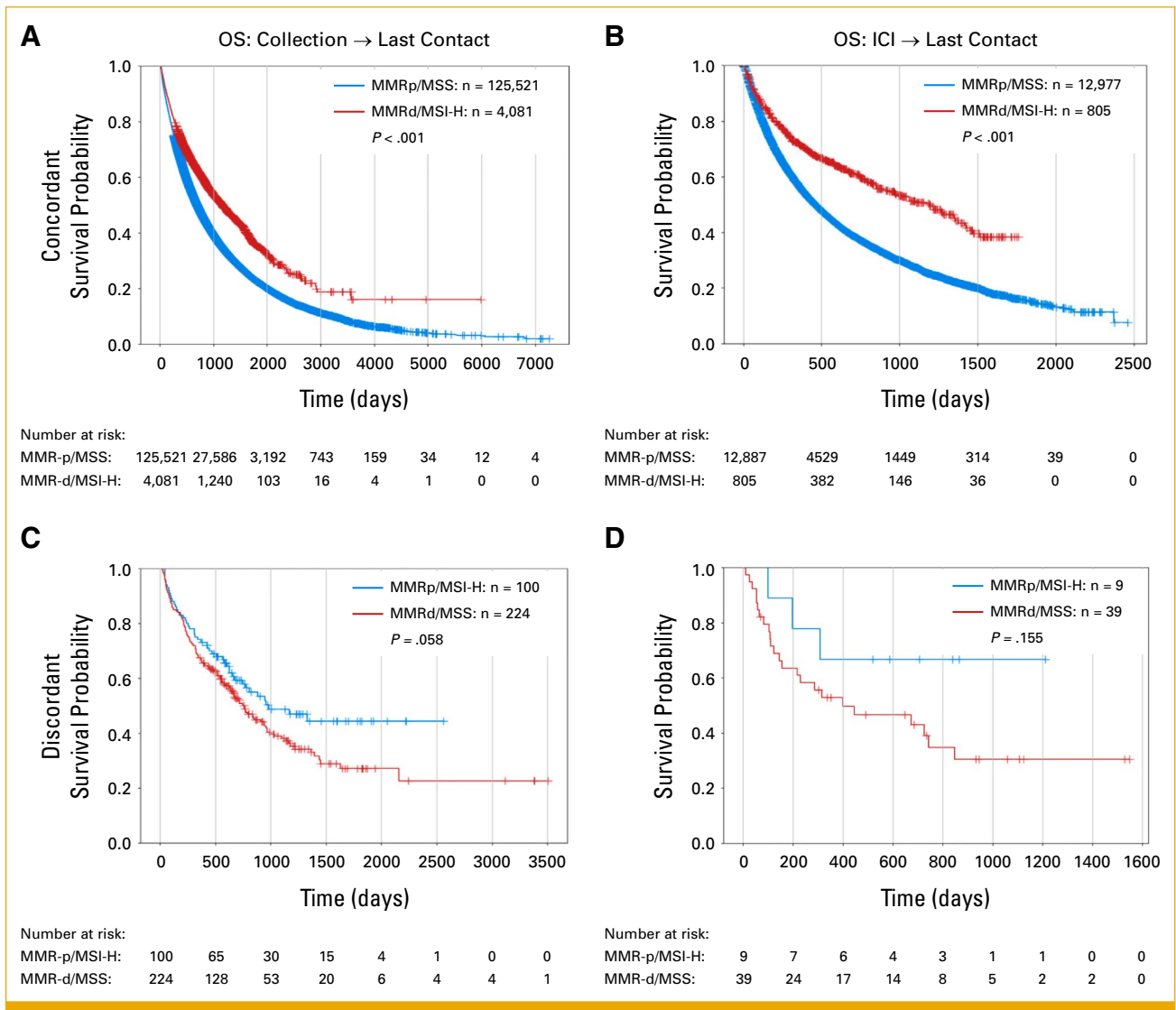
FIG 4. Overall survival (A, C) and time from immune checkpoint inhibitor to last contact (B, D) for concordant MMRd/MSI-H tumors as compared with MMRp/MSS (A, B) and discordant MMRp/MSI-H and MSS-MMRd tumors (C, D). Tumors included in this analysis are a subset of those in the main text who had matched insurance claim data available. HR was calculated using the Cox proportional hazards model, and P values were calculated using the log-rank test. HR, hazard ratio; ICI, immune checkpoint inhibitor; MMRd, mismatch repair deficient; MMRp, mismatch repair proficient; MSS, microsatellite stable; MSI-H, microsatellite instability high; OS, overall survival.

tumors frequently express a high neoantigen burden, making them immunogenic and responsive to ICI.[15,27-29] As a result, classification of tumors as MSI-H or MSS has become increasingly important due to its association with immunotherapy response across multiple tumor types.[10,30]

Previously published work in CRC comparing PCR-MSI with IHC showed concordance of 97.8% (132/136) among MSI-H cases and 97.9% (444/447) among MSS cases.[31] This is similar to the concordance we observed in MSI-H (97.44%, 168/6,913) and MSS CRC cases (99.90%, 26,147/26,172). Another study[14] showed that of 443 MSI-H cases with matching IHC, 32 cases were discordant (7.2%). We observed

a slightly lower discordance rate (2.6%), in agreement with several other studies.[7,12,13,32]

Interobserver variability (rate of agreement between multiple observers) found in the CPR (percent of discordant tumors whose diagnosis changed following CPR) is in line with that reported in the literature (>90%)[33] but was lower than expected in GE, SB, and EC MMRp/MSI-H tumors. Increased interobserver variability in MMRp/MSI-H discordant tumors makes sense as the reinterpretation of just one of the stains as deficient would trigger a change in diagnosis. It is unclear why the interobserver variability is lower in GE SB and EC but not CRC tumors. Future studies should seek to reproduce this phenomenon. Additionally, it

would be helpful to create guidelines for when an ambiguous IHC-MMR stain should undergo reflexive NGS testing.

NGS is a widely used technology that facilitates personalized cancer therapy by assaying for actionable genomic alterations, including single nucleotide variants, copy number variants, and structural variants in a single assay. NGS has been adapted for the purpose of MSI testing[12,34,35] and allows for a one-step approach to reporting MSI status along with other biomarkers. However, IHC and PCR-based assays performed on tumor tissue samples is preferred over NGS in determination of MSI/dMMR status. We demonstrate the value of assaying for MSI through orthogonal techniques (NGS-MSI and IHC) to trigger re-evaluation of discordant tumors by a pathologist. On the basis of our data, 1,111 patients would need to receive NGS-MSI testing to identify one patient as MSI-H that MMR-IHC would not have identified and 476 patients would need to receive MMR-IHC testing to identify one patient as MMR-d that NGS-MSI would not have identified.

Next, possible reasons for discordance in MMRp/MSI-H tumors were investigated. Missense mutations in assayed MMR protein that can cause the protein to be expressed but nonfunctional were considered (group 1) in addition to mutations in alternative MMR genes that were not stained for (*MLH3*, *MSH3*, *PMS1*; group 2). Finally, *POLE* mutations (group 3), which are associated with a hypermutated status,[37-42] were evaluated. Of the 83 MMRp/MSI-H tumors that underwent pathology review, 55.4% (46/83) had at least one Group 1, 2, or 3 mutation present. This highlights an advantage of assaying for MSI via NGS as compared with IHC, which is unable to identify MSI caused by alternations outside of the routinely tested four MMR genes.

It has been shown that nonpathogenic mutations in MLH1 can be responsible for discordance between NGS-MSI and IHC-MMR.[23] The two benign variants identified previously (p.V384D and p.A441T) were not observed in our data set. However, three additional nonpathogenic mutations were identified as possibly contributing to the observed discordance (p.E717D, p.L296S, and p.M242V). These

nonpathogenic mutations may result in false-positive results on IHC-MMR but not when using NGS-MSI.

For CRC, EG/SB, and EC tumors, MMRp/MSI-H tumors have higher prevalence of the TMB-H as compared with MMRd/MSS. These data suggest that high TMB correlates better with NGS-defined MSI-H compared with MMR deficiency defined by IHC and that these tumors may behave more like microsatellite instable tumors as compared with MSS/MMRd tumors. In CRC, MMRd/MSI-H tumors had a significantly higher TMB-H prevalence as compared with both MMRp/MSS and MMRp/MSI-H. This provides further evidence to support the hypothesis that MMRp/MSI-H cases should be considered eligible for ICI therapy and aligns with previous studies that showed 82% of MSI-H tumors were also TMB-H.[43]

The overall survival and IO therapy associated survival of MSI-H/MMRp tumors was noninferior to MSS/MMRd tumors. This further bolsters the argument that NGS-MSI is equivalent and at best provides several advantages when used in conjunction with IHC-MMR. Furthermore, these findings are hypothesis-generating for the concept that, in cases of discordance between MMR and NGS, MSI-NGS is a better predictive biomarker for response to ICI.

One of the limitations of our study is that it was retrospective. Additionally, tumors that undergo NGS tend to of an advanced stage or has undergone treatment before sequencing. Furthermore, *MLH1* promoter hypermethylation status was not available.[25] No data on the germline status of MMR gene were available so patients in our data set with Lynch syndrome were unable to be identified. Further validation of these data should be done for early-stage tumors.

Despite the limitations, from a clinical standpoint, if there is one potential biomarker for which curative responses can be seen across tumor types, it is mismatch repair deficiency. Although, importantly, other pan-tumor biomarkers exist (NTRK1/2/3 fusions, RET fusions, and TMB-H). As a result, these opportunities should not be missed. As NGS-based testing is increasingly adopted with more guidelines endorsing it, these clinically relevant discordances will occur more frequently.

AFFILIATIONS

[1]University of Michigan, Ann Arbor, MI
[2]Caris Life Sciences, Phoenix, AZ
[3]Karmanos Cancer Institute, Detroit, MI
[4]Wayne State University School of Medicine, Detroit, MI
[5]Women & Infants Hospital/Alpert Medical School of Brown University, Providence, RI
[6]University of Cincinnati Medical Center, Cincinnati, OH
[7]UC Davis Medical Center, Sacramento, CA
[8]University of Minnesota Masonic Cancer Center, Minneapolis, MN
[9]New York-Presbyterian/Weill Cornell Medical Center, New York, NY
[10]Fox Chase Cancer Center, Philadelphia, PA

CORRESPONDING AUTHOR

Rouba Ali-Fehmi, MD; e-mail: Alifehmi@med.umich.edu.

AUTHOR CONTRIBUTIONS

Conception and design: Rouba Ali-Fehmi, Harris Benjamin Krause, Robert T. Morris, Mira Kheil, Fadi Zaiem, Emmanuel S. Antonarakis,

Pashtoon Murtaza Kasi, Shuanzeng Wei, David Spetzler, Jim Abraham, George Sledge, Matthew J. Oberley, David Bryant

Administrative support: Milan Radovich, Matthew J. Oberley

Provision of study materials or patients: M. Ruhul Quddus, Jeffrey Swensen

Collection and assembly of data: Rouba Ali-Fehmi, Harris Benjamin Krause, Robert T. Morris, Logan Corey, Sudeshna Bandyopadhyay, Mira Kheil, Leana Elbashir, M. Ruhul Quddus, Evi Abada, Emmanuel S. Antonarakis, David Spetzler, Jim Abraham, Matthew J. Oberley, David Bryant

Data analysis and interpretation: Rouba Ali-Fehmi, Harris Benjamin Krause, Robert T. Morris, John J. Wallbillich, Logan Corey, Leana Elbashir, Thomas Herzog, Anthony N. Karnezis, Pashtoon Murtaza Kasi, Jeffrey Swensen, Andrew Elliott, Joanne Xiu, Jaclyn Hechtman, David Spetzler, Jim Abraham, Milan Radovich, George Sledge, Matthew J. Oberley

Manuscript writing: All authors

Final approval of manuscript: All authors

Accountable for all aspects of the work: All authors

AUTHORS' DISCLOSURES OF POTENTIAL CONFLICTS OF INTEREST

REFERENCES

1. Li GM: Mechanisms and functions of DNA mismatch repair. Cell Res 18:85-98, 2008
2. Reference deleted
3. Bonneville R, Krook MA, Chen HZ, et al: Detection of microsatellite instability biomarkers via next-generation sequencing. Methods Mol Biol 2055:119-132, 2020
4. Saul M, Poorman K, Tae H, et al: Population bias in somatic measurement of microsatellite instability status. Cancer Med 9:6452-6460, 2020
5. Riedinger CJ, Esnakula A, Haight PJ, et al: Characterization of mismatch-repair/microsatellite instability-discordant endometrial cancers. Cancer 130:385-399, 2024
6. Xiao J, Li W, Huang Y, et al: A next-generation sequencing-based strategy combining microsatellite instability and tumor mutation burden for comprehensive molecular diagnosis of advanced colorectal cancer. BMC Cancer 21:282, 2021
7. Shimozaki K, Hayashi H, Tanishima S, et al: Concordance analysis of microsatellite instability status between polymerase chain reaction based testing and next generation sequencing for solid tumors. Sci Rep 11:20003, 2021
8. Zito Marino F, Amato M, Ronchi A, et al: Microsatellite status detection in gastrointestinal cancers: PCR/NGS is mandatory in negative/patchy MMR immunohistochemistry. Cancers (Basel) 14:2204, 2022
9. Amemiya K, Hirotsu Y, Nagakubo Y, et al: Simple IHC reveals complex MMR alternations than PCR assays: Validation by LCM and next-generation sequencing. Cancer Med 11:4479-4490, 2022
10. Le DT, Durham JN, Smith KN, et al: Mismatch repair deficiency predicts response of solid tumors to PD-1 blockade. Science 357:409-413, 2017
11. Bartley AN, Mills AM, Konnick E, et al: Mismatch repair and microsatellite instability testing for immune checkpoint inhibitor therapy: Guideline from the College of American pathologists in collaboration with the association for molecular pathology and fight colorectal cancer. Arch Pathol Lab Med 146:1194-1210, 2022
12. Zhu L, Huang Y, Fang X, et al: A novel and reliable method to detect microsatellite instability in colorectal cancer by next-generation sequencing. J Mol Diagn 20:225-231, 2018
13. Middha S, Zhang L, Nafa K, et al: Reliable pan-cancer microsatellite instability assessment by using targeted next-generation sequencing data. JCO Precis Oncol 10.1200/PO.17.00084
14. Hechtman JF, Rana S, Middha S, et al: Retained mismatch repair protein expression occurs in approximately 6% of microsatellite instability-high cancers and is associated with missense mutations in mismatch repair genes. Mod Pathol 33:871-879, 2020
15. Vanderwalde A, Spetzler D, Xiao N, et al: Microsatellite instability status determined by next-generation sequencing and compared with PD-L1 and tumor mutational burden in 11,348 patients. Cancer Med 7:746-756, 2018
16. Marabelle A, Fakih M, Lopez J, et al: Association of tumour mutational burden with outcomes in patients with advanced solid tumours treated with pembrolizumab: Prospective biomarker analysis of the multicohort, open-label, phase 2 KEYNOTE-158 study. Lancet Oncol 21:1353-1365, 2020
17. Merino DM, McShane LM, Fabrizio D, et al: Establishing guidelines to harmonize tumor mutational burden (TMB): In silico assessment of variation in TMB quantification across diagnostic platforms: phase I of the friends of cancer research TMB harmonization project. J Immunother Cancer 8:e000147, 2020
18. Vega DM, Yee LM, McShane LM, et al: Aligning tumor mutational burden (TMB) quantification across diagnostic platforms: Phase II of the friends of cancer research TMB harmonization project. Ann Oncol 32:1626-1636, 2021
19. Abraham JP, Magee D, Cremolini C, et al: Clinical validation of a machine-learning–derived signature predictive of outcomes from first-line oxaliplatin-based chemotherapy in advanced colorectal cancer. Clin Cancer Res 27:1174-1183, 2021
20. You JF, Buhard O, Ligtenberg MJL, et al: Tumours with loss of MSH6 expression are MSI-H when screened with a pentaplex of five mononucleotide repeats. Br J Cancer 103:1840-1845, 2010
21. Verma L, Kane MF, Brassett C, et al: Mononucleotide microsatellite instability and germline MSH6 mutation analysis in early onset colorectal cancer. J Med Genet 36:678-682, 1999
22. Wu Y, Berends MJ, Mensink RG, et al: Association of hereditary nonpolyposis colorectal cancer-related tumors displaying low microsatellite instability with MSH6 germline mutations. Am J Hum Genet 65:1291-1298, 1999
23. Bosch DE, Yeh MM, Salipante SJ, et al: Isolated MLH1 loss by immunohistochemistry because of benign germline MLH1 polymorphisms. JCO Precis Oncol 10.1200/PO.22.00227
24. Boland CR, Goel A: Microsatellite instability in colorectal cancer. Gastroenterology 138:2073-2087.e3, 2010
25. Kato A, Sato N, Sugawara T, et al: Isolated loss of PMS2 immunohistochemical expression is frequently caused by heterogenous MLH1 promoter hypermethylation in Lynch syndrome screening for endometrial cancer patients. Am J Surg Pathol 40:770-776, 2016
26. Roudko V, Cimen Bozkus C, Greenbaum B, et al: Lynch syndrome and MSI-H cancers: From mechanisms to "off-the-shelf" cancer vaccines. Front Immunol 12:757804, 2021
27. Finotello F, Mayer C, Plattner C, et al: Molecular and pharmacological modulators of the tumor immune contexture revealed by deconvolution of RNA-seq data. Genome Med 11:34, 2019
28. Chang L, Chang M, Chang HM, et al: Microsatellite instability: A predictive biomarker for cancer immunotherapy. Appl Immunohistochem Mol Morphol 26:e15-e21, 2018
29. Kloor M, von Knebel Doeberitz M: The immune biology of microsatellite-unstable cancer. Trends Cancer 2:121-133, 2016
30. De Mattos-Arruda L, Siravegna G: How to use liquid biopsies to treat patients with cancer. ESMO Open 6:100060, 2021
31. Loughrey MB, McGrath J, Coleman HG, et al: Identifying mismatch repair-deficient colon cancer: Near-perfect concordance between immunohistochemistry and microsatellite instability testing in a large, population-based series. Histopathology 78:401-413, 2021
32. Malapelle U, Parente P, Pepe F, et al: Impact of pre-analytical factors on MSI test accuracy in mucinous colorectal adenocarcinoma: A multi-assay concordance study. Cells 9:2019, 2020
33. Sari A, Pollett A, Eiriksson LR, et al: Interobserver agreement for mismatch repair protein immunohistochemistry in endometrial and nonserous, nonmucinous ovarian carcinomas. Am J Surg Pathol 43:591-600, 2019
34. Hempelmann JA, Scroggins SM, Pritchard CC, et al: MSIplus for integrated colorectal cancer molecular testing by next-generation sequencing. J Mol Diagn 17:705-714, 2015
35. Waalkes A, Smith N, Penewit K, et al: Accurate pan-cancer molecular diagnosis of microsatellite instability by single-molecule molecular inversion probe capture and high-throughput sequencing. Clin Chem 64:950-958, 2018
36. Reference deleted
37. Ma X, Dong L, Liu X, et al: POLE/POLD1 mutation and tumor immunotherapy. J Exp Clin Cancer Res 41:216, 2022
38. Roberts SA, Gordenin DA: Hypermutation in human cancer genomes: Footprints and mechanisms. Nat Rev Cancer 14:786-800, 2014
39. Briggs S, Tomlinson I: Germline and somatic polymerase ε and δ mutations define a new class of hypermutated colorectal and endometrial cancers. J Pathol 230:148-153, 2013
40. Howitt BE, Shukla SA, Sholl LM, et al: Association of polymerase e-mutated and microsatellite-instable endometrial cancers with neoantigen load, number of tumor-infiltrating lymphocytes, and expression of PD-1 and PD-L1. JAMA Oncol 1:1319-1323, 2015
41. van Gool IC, Bosse T, Church DN: POLE proofreading mutation, immune response and prognosis in endometrial cancer. Oncoimmunology 5:e1072675, 2016
42. van Gool IC, Eggink FA, Freeman-Mills L, et al: POLE proofreading mutations elicit an antitumor immune response in endometrial cancer. Clin Cancer Res 21:3347-3355, 2015
43. Goodman AM, Sokol ES, Frampton GM, et al: Microsatellite-stable tumors with high mutational burden benefit from immunotherapy. Cancer Immunol Res 7:1570-1573, 2019
44. OMIM: An Online Catalog of Human Genes and Genetic Disorders. https://www.omim.org/

APPENDIX 1. NEXT-GENERATION SEQUENCING-592 GENE PANEL/WHOLE-EXOME SEQUENCING

NGS-592 or whole-exome sequencing (WES) was performed for 191,767 solid tumors (colorectal carcinoma [CRC]: n = 28,105, gastroesophageal [GE]: n = 9,849, small bowel [SB]: n = 1,405, endometrial carcinoma [EC]: n = 14,129) sequenced at Caris Life Sciences; both assays were internally validated at Caris Life Sciences, and there was high concordance between the two assays. Briefly, a concordance study comparing the WES panel with Caris' previously validated test NGS-592 panel included 113 samples that spanned 18 different lineages and covered a wide range of tumor cells density (20%-90% tumor nuclei) and variants frequency (8%-100%). Additionally, a concordance study comparing WES with an independently validated WES assay performed at TGen, included 65 samples of the 113 listed above, which spanned 16 different lineages and covered a wide range of tumor cells density (30%-90% tumor nuclei) and variant frequency (8%-94%). Both studies found these assays highly concordant.

Before molecular testing, tumor enrichment was achieved by harvesting targeted tissue using manual microdissection techniques. For NGS-592, genomic DNA was isolated from formalin-fixed paraffin-embedded (FFPE) sample using a DNA-QIAamp DNA FFPE Tissue Kit (Qiagen, Hilden, Germany). Tumor samples were sequenced using the NextSeq platform (Illumina, Inc, San Diego, CA). Matched normal tissue was not sequenced. A KAPA Library Quantification Kit (Agilent SureSelect XT-LI Library Preparation Kit, Agilent, Santa Clara, CA) was used in addition to a custom-designed SureSelect XT assay to enrich 592 whole-gene targets (Agilent Technologies). A list of the gene targets can be found in Appendix Table A1.

WES was performed on genomic DNA isolated from a micro-dissected, FFPE tumor sample. Genomic DNA was isolated from FFPE sample using a DNA-QIAamp DNA FFPE Tissue Kit (Qiagen) and sequenced using the Illumina NovaSeq 6,000 sequencers (Illumina, Inc). A KAPA Library Quantification Kit (Agilent SureSelect XT-LI Library Preparation Kit) was used in addition to a hybrid pull-down panel of baits designed to enrich for 720 clinically relevant genes at high coverage and high read-depth was used (Appendix Table A2), along with another panel designed to enrich for an additional >20,000 genes at lower depth. The performance of the WES assay was validated for sequencing variants, copy number alteration, tumor mutational burden (TMB), and microsatellite instability (MSI). The WES assay was validated to 50 ng of input and had a positive predictive value of 0.99 against a previously validated NGS assay. WES can detect variants in samples with tumor nuclei as low as 20% and detects down to 5% variant frequency with an average depth of at least 500×. A list of which portion of the genome were sequenced for PMS2, MSH6, MSH2, and MLH1 genes can be found in Appendix Table A3. MLH1 promoter hypermethylation status was not evaluated.

APPENDIX 2. IDENTIFICATION OF GENETIC VARIANTS

Genetic somatic variants identified were interpreted by board-certified molecular geneticists and categorized as pathogenic, likely pathogenic, variant of unknown significance, likely benign, or benign, according to the American College of Medical Genetics and Genomics (ACMG) standards and using the following databases: COSMIC, University of California, Santa Cruz (UCSC) Genome Brower, PubMed, HGMD, Genome Aggregation Database, ClinVar database, dbSNP database, InSiGHT database, IARC TP53 database, LOVD databases, BRCA Exchange, GeneReviews, Atlas of Genetics and Cytogenetics in Oncology and Hematology, CIViC database, cBioPortal, OMIM database,[44] and COSMIC Fusions. If a variant has a rs number associated with it, the dbSNP database must also be consulted to determine minor allele frequency of the mutation and based on the Standards and Guidelines for the Interpretation of Sequence Variants: A Joint Consensus Recommendation of the ACMG and the Association for Molecular Pathology. When assessing mutation frequencies of individual genes, pathogenic, and likely pathogenic were counted as mutations while benign, likely benign variants and variants of unknown significance were excluded unless otherwise noted. A list of variants considered pathogenic/likely pathogenic for PMS2, MSH6, MSH2, and MLH1 can be found in Appendix Table A4. The DNA aligner used was BWA 0.7.17, and variant calling was done using smatools mpileup + Pindel.

APPENDIX 3. MSI DETECTION AND CLASSIFICATION IN WES: METHODOLOGY AND CRITERIA

MSI by WES was examined by the direct analysis of 7,317 known homopolymer through pentapolymer target microsatellite regions sequenced in the WES gene panel and compared with the reference genome hg19 from the UCSC Genome Browser database. The number of microsatellite loci that were altered by somatic insertion or deletion was counted for each sample. Only insertions or deletions that result in increased or decreased number of tandem repeats were considered. Genomic variants in the microsatellite loci were detected using the same depth and frequency criteria as used for mutation detection. The threshold for microsatellite instability high (MSI-H) by WES was determined to be 116 or more loci with insertions or deletions, equivocal to be 113-115, and stable to be 112 or less.

APPENDIX 4. RNA EXTRACTION AND SEQUENCING METHODOLOGY FOR FFPE SPECIMENS

FFPE specimens underwent pathology review to estimate percent tumor content and tumor size; a minimum of 10% of tumor content in the area for microdissection was required to enable enrichment and extraction of tumor-specific RNA. RNA-RNeasy RNA FFPE Tissue Kit (Qiagen) was used, and RNA quality and quantity was determined using the Agilent TapeStation (Agilent Technologies). Biotinylated RNA baits were hybridized to the synthesized and purified cDNA targets and the bait-target complexes were amplified in a post-capture PCR reaction. The resultant libraries were quantified and normalized, and the pooled libraries were denatured, diluted, and sequenced using the Illumina NovaSeq platform (Illumina, Inc). Aligning of RNA sequences was done using STAR V.2.7.8a. For transcript counting, transcripts per million molecules were generated using the Salmon expression pipeline. Immune cell fraction was calculated via deconvolution of WTS data by quanTIseq.[27]

APPENDIX 5. PATTERNS OF MMR PROTEIN LOSS IN MSS AND MMRD TUMORS

Of the 21 mismatch repair deficient (MMRd)/microsatellite stable (MSS) GE tumors, 48% (10/21) were single losses (seven PMS2 and three MSH6 loss). There was one tumor that had loss of both MSH2 and MSH6 and another tumor had loss of both MLH1 and MSH6 (loss of one part of each of the heterodimers). Forty-three percent (9/21) of tumors had loss of both MLH1 and PMS2. All (3/3) of the SB tumors had only one loss (two tumors had loss of PMS2 and one had loss of MSH6).

In EC tumors, 15 of 46 had loss of MLH1, 25 of 46 had PMS2 loss, 2 of 46 had MSH2 loss, and 21 of 46 had MSH6 loss. Of the 17 tumors that had loss of two MMR proteins, 15 of 17 had loss of both proteins in the MLH1/PMS2 heterodimer. Two tumors had loss of both proteins in the MSH2/MSH6 heterodimer.

APPENDIX 6. TMB AND THE TUMOR IMMUNE MICROENVIRONMENT OF DISCORDANT CASES

When concordant tumors were investigated, MMRd/MSS CRC, EG/SB, and EC tumors had a significantly lower rate of TMB-H than mismatch repair proficient (MMRp)/MSI-H tumors (CRC: 12.5% TMB-H, n = 24 [mean = 29.5 mut/Mb, median = 6.5, range, 2-513] v 89.1% TMB-H, n = 46 [mean = 55.7 mut/Mb, median = 36.5, range, 5-327], P < .001; GE/SB: 37.5% TMB-H, n = 24 [mean = 23.5 mut/Mb, median = 8, range, 1-336] v 100% TMB-H, n = 7 [mean = 107.1 mut/Mb, median = 28, range: 10-579], P = .003; EC: 56.5% TMB-H, n = 46 [mean = 55.1 mut/Mb, median = 12, range: 1-324] v 86.2%, n = 29 [mean = 160.6 mut/Mb, median = 27, range: 6-520], P = .011; Fig 3A).

The prevalence of TMB-H in CRC discordant tumors was compared with concordant tumors. The magnitude of difference was the largest between MSS versus MSI-H tumors regardless of MMR status (MMRd/MSS: 12.5%, n = 24 [mean = 29.5 mut/Mb, median = 6.5, range, 2-513]; MMRp/MSS: 3.1%, n = 12,543 [mean = 6.9 mut/Mb, median = 6, range, 0-569]; MMRp/MSI-H 89.1%, n = 46 [mean = 55.7 mut/Mb, median = 36.5, range, 5-327]; MMRd/MSI-H 99.7%, n = 866 [mean = 40.8 mut/Mb, median = 36, range, 5-535]; P < .001 for all comparisons). MMRd/MSI-H had a significantly higher TMB-H prevalence than MMRp/MSS, and MMRp/MSI-H had a significantly lower TMB-H prevalence as compared with MMRd/MSI-H (Fig 3B). Similar results are observed for TMB-H prevalence in GE/SB (MMRp/MSS: 5.3%, n = 4,717 [mean = 6.8 mut/Mb, median = 6, range, 0-89]; MMRd/MSI-H: 97.4%, n = 114 [mean = 29.6 mut/Mb, median = 27, range, 9-231) and EC (MMRp/MSS: 4.1%, n = 12,224 [mean = 9.1 mut/Mb, median = 6, range, 0-554]; MMRd/MSI-H: 96.1%, n = 2,806 [mean = 29.4 mut/Mb, median = 20, range, 4-678]).

TABLE A1. Gene List for Targeted DNA Sequencing Panel

Genes
ABI1 (10p12.1)
ABL1 (9q34.12)
ABL2 (1q25.2)
ACKR3 (2q37.3)
ACSL3 (2q36.1)
ACSL6 (5q31.1)
ADGRA2 (8p11.23)
AFDN (6q27)
AFF1 (4q21.3-22.1)
AFF3 (2q11.2)
AFF4 (5q31.1)
AKAP9 (7q21.2)
AKT1 (14q32.33)
AKT2 (19q13.2)
AKT3 (1q43-44)
ALDH2 (12q24.12)
ALK (2p23.2-23.1)
AMER1 (Xq11.2)
APC (5q22.2)
AR (Xq12)
ARAF (Xp11.3)
ARFRP1 (20q13.33)
ARHGAP26 (5q31.3)
ARHGEF12 (11q23.3)
ARID1A (1p36.11)
ARID2 (12q12)
ARNT (1q21.3)
ASPSCR1 (17q25.3)
ASXL1 (20q11.21)
ATF1 (12q13.12)
ATIC (2q35)
ATM (11q22.3)
ATP1A1 (1p13.1)
ATP2B3 (Xq28)
ATR (3q23)
ATRX (Xq21.1)
AURKA (20q13.2)
AURKB (17p13.1)
AXIN1 (16p13.3)
AXL (19q13.2)
BAP1 (3p21.1)
BARD1 (2q35)
BCL10 (1p22.3)
BCL11A (2p16.1)
BCL11B (14q32.2)
BCL2 (18q21.33)
BCL2L11 (2q13)
BCL2L2 (14q11.2)
BCL3 (19q13.32)
BCL6 (3q27.3)
BCL7A (12q24.31)

(continued in next column)

TABLE A1. Gene List for Targeted DNA Sequencing Panel (continued)

Genes
BCL9 (1q21.2)
BCOR (Xp11.4)
BCORL1 (Xq26.1)
BCR (22q11.23)
BIRC3 (11q22.2)
BLM (15q26.1)
BMPR1A (10q23.2)
BRAF (7q34)
BRCA1 (17q21.31)
BRCA2 (13q13.1)
BRD3 (9q34.2)
BRD4 (19p13.12)
BRIP1 (17q23.2)
BTG1 (12q21.33)
BTK (Xq22.1)
BUB1B (15q15.1)
C15orf65 (15q21.3)
CACNA1D (3p21.1)
CALR (19p13.13)
CAMTA1 (1p36.31-36.23)
CANT1 (17q25.3)
CARD11 (7p22.2)
CARS1 (11p15.4)
CASP8 (2q33.1)
CBFA2T3 (16q24.3)
CBFB (16q22.1)
CBL (11q23.3)
CBLB (3q13.11)
CBLC (19q13.32)
CCDC6 (10q21.2)
CCN6 (6q21)
CCNB1IP1 (14q11.2)
CCND1 (11q13.3)
CCND2 (12p13.32)
CCND3 (6p21.1)
CCNE1 (19q12)
CD274 (9p24.1)
CD74 (5q33.1)
CD79A (19q13.2)
CD79B (17q23.3)
CDC73 (1q31.2)
CDH1 (16q22.1)
CDH11 (16q21)
CDK12 (17q12)
CDK4 (12q14.1)
CDK6 (7q21.2)
CDK8 (13q12.13)
CDKN1B (12p13.1)
CDKN2A (9p21.3)
CDKN2B (9p21.3)
CDKN2C (1p32.3)

(continued on following page)

TABLE A1. Gene List for Targeted DNA Sequencing Panel (continued)

Genes
CDX2 (13q12.2)
CEBPA (19q13.11)
CHCHD7 (8q12.1)
CHEK1 (11q24.2)
CHEK2 (22q12.1)
CHIC2 (4q12)
CHN1 (2q31.1)
CIC (19q13.2)
CIITA (16p13.13)
CLP1 (11q12.1)
CLTC (17q23.1)
CLTCL1 (22q11.21)
CNBP (3q21.3)
CNOT3 (19q13.42)
CNTRL (9q33.2)
COL1A1 (17q21.33)
COPB1 (11p15.2)
COX6C (8q22.2)
CREB1 (2q33.3)
CREB3L1 (11p11.2)
CREB3L2 (7q33)
CREBBP (16p13.3)
CRKL (22q11.21)
CRLF2 (Xp22.33)
CRTC1 (19p13.11)
CRTC3 (15q26.1)
CSF1R (5q32)
CSF3R (1p34.3)
CTCF (16q22.1)
CTLA4 (2q33.2)
CTNNA1 (5q31.2)
CTNNB1 (3p22.1)
CYLD (16q12.1)
CYP2D6 (22q13.2)
DAXX (6p21.32)
DDB2 (11p11.2)
DDIT3 (12q13.3)
DDR2 (1q23.3)
DDX10 (11q22.3)
DDX5 (17q23.3)
DDX6 (11q23.3)
DEK (6p22.3)
DICER1 (14q32.13)
DNM2 (19p13.2)
DNMT3A (2p23.3)
DOT1L (19p13.3)
EBF1 (5q33.3)
ECT2L (6q24.1)
EGFR (7p11.2)
EIF4A2 (3q27.3)
ELF4 (Xq26.1)

TABLE A1. Gene List for Targeted DNA Sequencing Panel (continued)

Genes
ELK4 (1q32.1)
ELL (19p13.11)
ELN (7q11.23)
EML4 (2p21)
EMSY (11q13.5)
EP300 (22q13.2)
EPHA3 (3p11.1)
EPHA5 (4q13.1-13.2)
EPHB1 (3q22.2)
EPS15 (1p32.3)
ERBB2 (17q12)
ERBB3 (12q13.2)
ERBB4 (2q34)
ERC1 (12p13.33)
ERCC1 (19q13.32)
ERCC2 (19q13.32)
ERCC3 (2q14.3)
ERCC4 (16p13.12)
ERCC5 (13q33.1)
ERG (21q22.2)
ESR1 (6q25.1-25.2)
ETV1 (7p21.2)
ETV4 (17q21.31)
ETV5 (3q27.2)
ETV6 (12p13.2)
EWSR1 (22q12.2)
EXT1 (8q24.11)
EXT2 (11p11.2)
EZH2 (7q36.1)
EZR (6q25.3)
FANCA (16q24.3)
FANCC (9q22.32)
FANCD2 (3p25.3)
FANCE (6p21.31)
FANCF (11p14.3)
FANCG (9p13.3)
FANCL (2p16.1)
FAS (10q23.31)
FBXO11 (2p16.3)
FBXW7 (4q31.3)
FCRL4 (1q23.1)
FEV (2q35)
FGF10 (5p12)
FGF14 (13q33.1)
FGF19 (11q13.3)
FGF23 (12p13.32)
FGF3 (11q13.3)
FGF4 (11q13.3)
FGF6 (12p13.32)
FGFR1 (8p11.23)
FGFR1OP (6q27)

TABLE A1. Gene List for Targeted DNA Sequencing Panel (continued)

Genes
FGFR2 (10q26.13)
FGFR3 (4p16.3)
FGFR4 (5q35.2)
FH (1q43)
FHIT (3p14.2)
FIP1L1 (4q12)
FLCN (17p11.2)
FLI1 (11q24.3)
FLT1 (13q12.3)
FLT3 (13q12.2)
FLT4 (5q35.3)
FNBP1 (9q34.11)
FOXA1 (14q21.1)
FOXL2 (3q22.3)
FOXO1 (13q14.11)
FOXO3 (6q21)
FOXO4 (Xq13.1)
FOXP1 (3p13)
FSTL3 (19p13.3)
FUBP1 (1p31.1)
FUS (16p11.2)
GAS7 (17p13.1)
GATA1 (Xp11.23)
GATA2 (3q21.3)
GATA3 (10p14)
GID4 (17p11.2)
GMPS (3q25.31)
GNA11 (19p13.3)
GNA13 (17q24.1)
GNAQ (9q21.2)
GNAS (20q13.32)
GOLGA5 (14q32.12)
GOPC (6q22.1)
GPC3 (Xq26.2)
GPHN (14q23.3-24.1)
GRIN2A (16p13.2)
GSK3B (3q13.33)
H3-3A (1q42.12)
H3-3B (17q25.1)
H3C2 (6p22.2)
H4C9 (6p22.1)
HERPUD1 (16q13)
HEY1 (8q21.13)
HGF (7q21.11)
HIP1 (7q11.23)
HLF (17q22)
HMGA1 (6p21.31)
HMGA2 (12q14.3)
HNF1A (12q24.31)
HNRNPA2B1 (7p15.2)
HOOK3 (8p11.21)

TABLE A1. Gene List for Targeted DNA Sequencing Panel (continued)

Genes
HOXA11 (7p15.2)
HOXA13 (7p15.2)
HOXA9 (7p15.2)
HOXC11 (12q13.13)
HOXC13 (12q13.13)
HOXD11 (2q31.1)
HOXD13 (2q31.1)
HRAS (11p15.5)
HSP90AA1 (14q32.31)
HSP90AB1 (6p21.1)
IDH1 (2q34)
IDH2 (15q26.1)
IGF1R (15q26.3)
IKBKE (1q32.1)
IKZF1 (7p12.2)
IL2 (4q27)
IL21R (16p12.1)
IL6ST (5q11.2)
IL7R (5p13.2)
INHBA (7p14.1)
IRF4 (6p25.3)
IRS2 (13q34)
ITK (5q33.3)
JAK1 (1p31.3)
JAK2 (9p24.1)
JAK3 (19p13.11)
JAZF1 (7p15.2-15.1)
JUN (1p32.1)
KAT6A (8p11.21)
KAT6B (10q22.2)
KCNJ5 (11q24.3)
KDM5A (12p13.33)
KDM5C (Xp11.22)
KDM6A (Xp11.3)
KDR (4q12)
KDSR (18q21.33)
KEAP1 (19p13.2)
KIAA1549 (7q34)
KIF5B (10p11.22)
KIT (4q12)
KLF4 (9q31.2)
KLHL6 (3q27.1)
KLK2 (19q13.33)
KMT2A (11q23.3)
KMT2C (7q36.1)
KMT2D (12q13.12)
KNL1 (15q15.1)
KRAS (12p12.1)
KTN1 (14q22.3)
LASP1 (17q12)
LCK (1p35.2)

TABLE A1. Gene List for Targeted DNA Sequencing Panel (continued)

Genes
LCP1 (13q14.13)
LGR5 (12q21.1)
LHFPL6 (13q13.3-14.11)
LIFR (5p13.1)
LMO1 (11p15.4)
LMO2 (11p13)
LPP (3q27.3-28)
LRIG3 (12q14.1)
LRP1B (2q22.1-22.2)
LYL1 (19p13.13)
MAF (16q23.2)
MAFB (20q12)
MALT1 (18q21.32)
MAML2 (11q21)
MAP2K1 (15q22.31)
MAP2K2 (19p13.3)
MAP2K4 (17p12)
MAP3K1 (5q11.2)
MAX (14q23.3)
MCL1 (1q21.2)
MDM2 (12q15)
MDM4 (1q32.1)
MDS2 (1p36.11)
MECOM (3q26.2)
MED12 (Xq13.1)
MEF2B (19p13.11)
MEN1 (11q13.1)
MET (7q31.2)
MITF (3p13)
MLF1 (3q25.32)
MLH1 (3p22.2)
MLLT1 (19p13.3)
MLLT10 (10p12.31)
MLLT11 (1q21.3)
MLLT3 (9p21.3)
MLLT6 (17q12)
MN1 (22q12.1)
MNX1 (7q36.3)
MPL (1p34.2)
MRE11 (11q21)
MRTFA (22q13.1-13.2)
MSH2 (2p21-16.3)
MSH6 (2p16.3)
MSI2 (17q22)
MSN (Xq12)
MTCP1 (Xq28)
MTOR (1p36.22)
MUC1 (1q22)
MUTYH (1p34.1)
MYB (6q23.3)
MYC (8q24.21)

(continued in next column)

TABLE A1. Gene List for Targeted DNA Sequencing Panel (continued)

Genes
MYCL (1p34.2)
MYCN (2p24.3)
MYD88 (3p22.2)
MYH11 (16p13.11)
MYH9 (22q12.3)
NACA (12q13.3)
NBN (8q21.3)
NCKIPSD (3p21.31)
NCOA1 (2p23.3)
NCOA2 (8q13.3)
NCOA4 (10q11.22)
NDRG1 (8q24.22)
NF1 (17q11.2)
NF2 (22q12.2)
NFE2L2 (2q31.2)
NFIB (9p23-22.3)
NFKB2 (10q24.32)
NFKBIA (14q13.2)
NIN (14q22.1)
NKX2-1 (14q13.3)
NONO (Xq13.1)
NOTCH1 (9q34.3)
NOTCH2 (1p12)
NPM1 (5q35.1)
NR4A3 (9q31.1)
NRAS (1p13.2)
NSD1 (5q35.3)
NSD2 (4p16.3)
NSD3 (8p11.23)
NT5C2 (10q24.32-24.33)
NTRK1 (1q23.1)
NTRK2 (9q21.33)
NTRK3 (15q25.3)
NUMA1 (11q13.4)
NUP214 (9q34.13)
NUP93 (16q13)
NUP98 (11p15.4)
NUTM1 (15q14)
NUTM2B (10q22.3)
OLIG2 (21q22.11)
OMD (9q22.31)
P2RY8 (Xp22.33)
PAFAH1B2 (11q23.3)
PAK3 (Xq23)
PALB2 (16p12.2)
PATZ1 (22q12.2)
PAX3 (2q36.1)
PAX5 (9p13.2)
PAX7 (1p36.13)
PAX8 (2q14.1)
PBRM1 (3p21.1)

(continued on following page)

TABLE A1. Gene List for Targeted DNA Sequencing Panel (continued)

Genes
PBX1 (1q23.3)
PCM1 (8p22)
PCSK7 (11q23.3)
PDCD1 (2q37.3)
PDCD1LG2 (9p24.1)
PDE4DIP (1q21.2)
PDGFB (22q13.1)
PDGFRA (4q12)
PDGFRB (5q32)
PDK1 (2q31.1)
PER1 (17p13.1)
PHF6 (Xq26.2)
PHOX2B (4p13)
PICALM (11q14.2)
PIK3CA (3q26.32)
PIK3CG (7q22.3)
PIK3R1 (5q13.1)
PIK3R2 (19p13.11)
PIM1 (6p21.2)
PLAG1 (8q12.1)
PML (15q24.1)
PMS1 (2q32.2)
PMS2 (7p22.1)
POLE (12q24.33)
POT1 (7q31.33)
POU2AF1 (11q23.1)
POU5F1 (6p21.33)
PPARG (3p25.2)
PPP2R1A (19q13.41)
PRCC (1q23.1)
PRDM1 (6q21)
PRDM16 (1p36.32)
PRF1 (10q22.1)
PRKAR1A (17q24.2)
PRKDC (8q11.21)
PRRX1 (1q24.2)
PSIP1 (9p22.3)
PTCH1 (9q22.32)
PTEN (10q23.31)
PTPN11 (12q24.13)
PTPRC (1q31.3-32.1)
RABEP1 (17p13.2)
RAC1 (7p22.1)
RAD21 (8q24.11)
RAD50 (5q31.1)
RAD51 (15q15.1)
RAD51B (14q24.1)
RAF1 (3p25.2)
RALGDS (9q34.13-34.2)
RANBP17 (5q35.1)
RAP1GDS1 (4q23)

TABLE A1. Gene List for Targeted DNA Sequencing Panel (continued)

Genes
RARA (17q21.2)
RB1 (13q14.2)
RBM15 (1p13.3)
RECQL4 (8q24.3)
REL (2p16.1)
RET (10q11.21)
RHOH (4p14)
RICTOR (5p13.1)
RMI2 (16p13.13)
RNF213 (17q25.3)
RNF43 (17q22)
ROS1 (6q22.1)
RPL10 (Xq28)
RPL22 (1p36.31)
RPL5 (1p22.1)
RPN1 (3q21.3)
RPTOR (17q25.3)
RUNX1 (21q22.12)
RUNX1T1 (8q21.3)
SBDS (7q11.21)
SDC4 (20q13.12)
SDHAF2 (11q12.2)
SDHB (1p36.13)
SDHC (1q23.3)
SDHD (11q23.1)
SEPTIN5 (22q11.21)
SEPTIN6 (Xq24)
SEPTIN9 (17q25.3)
SET (9q34.11)
SETBP1 (18q12.3)
SETD2 (3p21.31)
SF3B1 (2q33.1)
SFPQ (1p34.3)
SH2B3 (12q24.12)
SH3GL1 (19p13.3)
SLC34A2 (4p15.2)
SLC45A3 (1q32.1)
SMAD2 (18q21.1)
SMAD4 (18q21.2)
SMARCA4 (19p13.2)
SMARCB1 (22q11.23)
SMARCE1 (17q21.2)
SMO (7q32.1)
SNX29 (16p13.13-13.12)
SOCS1 (16p13.13)
SOX10 (22q13.1)
SOX2 (3q26.33)
SPECC1 (17p11.2)
SPEN (1p36.21-36.13)
SPOP (17q21.33)
SRC (20q11.23)

TABLE A1. Gene List for Targeted DNA Sequencing Panel (continued)

Genes
SRGAP3 (3p25.3)
SRSF2 (17q25.1)
SRSF3 (6p21.31-21.2)
SS18 (18q11.2)
SS18L1 (20q13.33)
SSX1 (Xp11.23)
STAG2 (Xq25)
STAT3 (17q21.2)
STAT4 (2q32.2-32.3)
STAT5B (17q21.2)
STIL (1p33)
STK11 (19p13.3)
SUFU (10q24.32)
SUZ12 (17q11.2)
SYK (9q22.2)
TAF15 (17q12)
TAL1 (1p33)
TAL2 (9q31.2)
TBL1XR1 (3q26.32)
TCEA1 (8q11.23)
TCF12 (15q21.3)
TCF3 (19p13.3)
TCF7L2 (10q25.2-25.3)
TCL1A (14q32.13)
TENT5C (1p12)
TERT (5p15.33)
TET1 (10q21.3)
TET2 (4q24)
TFE3 (Xp11.23)
TFEB (6p21.1)
TFG (3q12.2)
TFPT (19q13.42)
TFRC (3q29)
TGFBR2 (3p24.1)
THRAP3 (1p34.3)
TLX1 (10q24.31)
TLX3 (5q35.1)
TMPRSS2 (21q22.3)
TNFAIP3 (6q23.3)
TNFRSF14 (1p36.32)
TNFRSF17 (16p13.13)
TOP1 (20q12)
TP53 (17p13.1)
TPM3 (1q21.3)
TPM4 (19p13.12-13.11)
TPR (1q31.1)
TRAF7 (16p13.3)
TRIM26 (6p22.1)
TRIM27 (6p22.1)
TRIM33 (1p13.2)
TRIP11 (14q32.12)

(continued in next column)

TABLE A1. Gene List for Targeted DNA Sequencing Panel (continued)

Genes
TRRAP (7q22.1)
TSC1 (9q34.13)
TSC2 (16p13.3)
TSHR (14q31.1)
TTL (2q14.1)
U2AF1 (21q22.3)
UBR5 (8q22.3)
USP6 (17p13.2)
VEGFA (6p21.1)
VEGFB (11q13.1)
VHL (3p25.3)
VTI1A (10q25.2)
WAS (Xp11.23)
WDCP (2p23.3)
WIF1 (12q14.3)
WRN (8p12)
WT1 (11p13)
WWTR1 (3q25.1)
XPA (9q22.33)
XPC (3p25.1)
XPO1 (2p15)
YWHAE (17p13.3)
ZBTB16 (11q23.2)
ZMYM2 (13q12.11)
ZNF217 (20q13.2)
ZNF331 (19q13.42)
ZNF384 (12p13.31)
ZNF521 (18q11.2)
ZNF703 (8p11.23)
ZRSR2 (Xp22.2)

TABLE A2. Gene List for the Subset of Whole Exome Panel Genes Sequenced at High Coverage and Read Depth

Genes
ABL1
ABRAXAS1
ACVR1
AIP
AKT1
AKT2
AKT3
ALK
AMER1
APC
AR
ARAF
ARID1A
ARID1B
ARID2
ASXL1
ATM
ATR
ATRX
AURKB
B2M
BAP1
BARD1
BCL2
BCOR
BCORL1
BLM
BMPR1A
BRAF
BRCA1
BRCA2
BRIP1
CARD11
CBFB
CCND1
CCND2
CCND3
CCNE1
CD274
CDC73
CDH1
CDK12
CDK4
CDK6
CDKN1B
CDKN1C
CDKN2A
CDKN2B

(continued in next column)

TABLE A2. Gene List for the Subset of Whole Exome Panel Genes Sequenced at High Coverage and Read Depth (continued)

Genes
CHEK1
CHEK2
CIC
CLYBL
CREBBP
CRKL
CSF1R
CTNNB1
CYLD
DAXX
DDR2
DICER1
DNMT3A
EGFR
EME1
EPCAM
EP300
EPHA2
ERBB2
ERBB3
ERBB4
ERCC2
ESR1
EZH2
FANCA
FANCB
FANCC
FANCD2
FANCE
FANCF
FANCG
FANCI
FANCL
FANCM
FAS
FAT1
FBXW7
FGF10
FGF19
FGF3
FGF4
FGFR1
FGFR2
FGFR3
FGFR4
FH
FLCN
FLT1

(continued on following page)

TABLE A2. Gene List for the Subset of Whole Exome Panel Genes Sequenced at High Coverage and Read Depth (continued)

Genes
FLT3
FLT4
FOXL2
FUBP1
FYN
GATA3
GLI2
GNA11
GNA13
GNAQ
GNAS
H3F3A
H3F3B
HIST1H3B
HNF1A
HRAS
ID2
IDH1
IDH2
JAK1
JAK2
JAK3
KAT6A
KDM5C
KDM6A
KDR
KIT
KLLN
KMT2A
KMT2C
KMT2D
KRAS
LCK
LYN
LZTR1
MAP2K1
MAP2K2
MAP2K4
MAP3K1
MAX
MDM2
MDM4
MEF2B
MEN1
MET
MITF
MLH1
MLH3

TABLE A2. Gene List for the Subset of Whole Exome Panel Genes Sequenced at High Coverage and Read Depth (continued)

Genes
MPL
MRE11
MSH2
MSH3
MSH6
MST1R
MTOR
MUTYH
MYB
MYC
MYCL
MYCN
NBN
NF1
NF2
NFKBIA
NOTCH1
NPM1
NRAS
NSD1
NTHL1
NTRK1
NTRK2
NTRK3
PALB2
PBRM1
PDCD1
PDCD1LG2
PDGFRA
PDGFRB
PER1
PHOX2B
PIK3CA
PIK3R1
PIM1
PMS1
PMS2
POLD1
POLE
POT1
PPARG
PPP2R1A
PRDM1
PRKAR1A
PRKDC
PTCH1
PTEN
PTPN11

TABLE A2. Gene List for the Subset of Whole Exome Panel Genes Sequenced at High Coverage and Read Depth (continued)

Genes
RAD50
RAD51C
RAD51D
RAF1
RB1
RET
RICTOR
RNF43
ROS1
RSPO1
RSPO2
RSPO3
RUNX1
SDHA
SDHAF2
SDHB
SDHC
SDHD
SETD2
SF3B1
SLX4
SMAD2
SMAD4
SMARCA4
SMARCB1
SMARCE1
SMO
SOCS1
SPEN
SPOP
SRC
STK11
SUFU
TERC
TMEM127
TNFAIP3
TNFRSF14
TOP1
TOP2A
TP53
TSC1
TSC2
U2AF1
UBR5
VHL
WRN
WT1
YAP1

TABLE A2. Gene List for the Subset of Whole Exome Panel Genes Sequenced at High Coverage and Read Depth (continued)

Genes
YES1
ZNRF3
ABL2
ACKR3
ACSL3
ACSL6
AFDN
AFF1
AFF3
ARNT
ATF1
ATIC
ATP1A1
BCL11A
BCL11B
BCL2L11
BCL2L2
BCL3
BCL6
BCL9
BRD4
BTG1
C15orf65
CACNA1D
CALR
CAMTA1
CARS
CASP8
CBL
CCDC6
CD74
CD79A
CDH11
CDK8
CDKN2C
CDX2
CEBPA
CHIC2
CLTCL1
CNBP
COX6C
CREB3L2
CRTC3
CTCF
CTNNA1
DDIT3
DDX41
DDX6

TABLE A2. Gene List for the Subset of Whole Exome Panel Genes Sequenced at High Coverage and Read Depth (continued)

Genes
DEK
EBF1
ECT2L
ELK4
EPHA3
ERCC1
ERCC3
ERG
ETV1
ETV5
ETV6
EWSR1
EXT1
EXT2
EZR
FAM46C
FCRL4
FGF23
FGFR1OP
FHIT
FLI1
FNBP1
FOXA1
FOXO1
FOXO3
FOXP1
FSTL3
FUS
GATA2
GID4
GMPS
GRIN2A
HEY1
HIST1H4I
HLF
HMGA2
HMGN2P46
HOOK3
HOXA11
HOXA13
HOXA9
HOXB13
HOXD13
HSP90AA1
HSP90AB1
IGF1R
IKZF1
IL7R

TABLE A2. Gene List for the Subset of Whole Exome Panel Genes Sequenced at High Coverage and Read Depth (continued)

Genes
IRF4
ITK
JAZF1
JUN
KAT6B
KCNJ5
KDSR
KIAA1549
KIF5B
KLF4
KLHL6
KLK2
LHFPL6
LIFR
LPP
LRP1B
MAF
MAML2
MCL1
MDS2
MECOM
MLF1
MLLT10
MLLT11
MLLT3
MN1
MSI2
MUC1
MYD88
NCOA2
NDRG1
NFIB
NFKB2
NIN
NKX2-1
NOTCH2
NR4A3
NUP214
NUP93
NUP98
NUTM1
OLIG2
PAFAH1B2
PAX3
PAX5
PAX8
PBX1
PCM1

TABLE A2. Gene List for the Subset of Whole Exome Panel Genes Sequenced at High Coverage and Read Depth (continued)

Genes
PDE4DIP
POU2AF1
PRCC
PRRX1
PTPRC
RAC1
RHOH
RMI2
RPL22
RPN1
RUNX1T1
SBDS
SDC4
SETBP1
SFPQ
SLC34A2
SNX29
SOX10
SOX2
SPECC1
SPRED1
SRGAP3
SRSF2
SRSF3
STAT3
STAT5B
STIL
SUZ12
SYK
TAF15
TBXT
TCEA1
TCF7L2
TERT
TET1
TFRC
TGFBR1
TGFBR2
THRAP3
TPM3
TPM4
TRIM27
TRRAP
TSHR
USP6
VTI1A
WDCP
WISP3

(continued in next column)

TABLE A2. Gene List for the Subset of Whole Exome Panel Genes Sequenced at High Coverage and Read Depth (continued)

Genes
WWTR1
XPC
YWHAE
ZBTB16
ZNF217
ZNF331
ZNF384
ZNF521
ABCB11
ACD
ACVR1B
ADGRA2
AJUBA
ALOX12B
ANKRD26
APLNR
ARFRP1
ARHGAP35
ARHGEF12
ARID5B
ASPSCR1
ASXL2
AURKA
AXIN1
AXIN2
AXL
BCL10
BCL2L1
BCL2L12
BIRC3
BRD3
BTG2
BTK
BUB1B
CBFA2T3
CBLB
CD22
CD70
CD79B
CDH23
CDKN1A
CHD2
CHD4
CHN1
CIITA
CNOT3
CREB1
CREB3L1

(continued on following page)

TABLE A2. Gene List for the Subset of Whole Exome Panel Genes Sequenced at High Coverage and Read Depth (continued)

Genes
CRLF2
CRTC1
CSF3R
CTLA4
CUL3
CUL4A
CUX1
CXCR4
CYP17A1
CYP2D6
DDB2
DDR1
DDX3X
DIS3
DIS3L2
DKC1
DMC1
DNA2
DNAJB1
DOT1L
EED
EGLN1
EIF1AX
EIF4A2
ELF3
ELOC
EME2
EML4
EMSY
EPHA5
EPHA7
EPHB1
EPHB4
ERC1
ERCC4
ERCC5
ERCC6
EREG
ERRFI1
ETS1
ETV4
EXO1
FAT3
FBXO11
FEN1
FGF12
FGF14
FGF6

Genes
FIP1L1
FOXO4
FRS2
GABRA6
GALNT12
GATA1
GATA4
GATA6
GEN1
GLI1
GOPC
GPC3
GPS2
GREM1
GRM3
GSK3B
H2AFX
HDAC1
HGF
HIF1A
HIST1H3C
HLA-A
HRG
HSD3B1
ID3
IFNGR1
IGF2
IKBKE
INHBA
INPP4B
IRF1
IRF2
IRS2
KDM5A
KEAP1
KEL
KIF1B
LDLR
LIG1
LMNA
LMO1
LMO2
LTK
MAFB
MAGI2
MALT1
MAP3K13
MAPK1

TABLE A2. Gene List for the Subset of Whole Exome Panel Genes Sequenced at High Coverage and Read Depth (continued)

Genes
MAPK3
MBD4
MDC1
MED12
MERTK
MGA
MGMT
MKNK1
MTAP
MTCP1
MUS81
MYH11
MYH9
NCOA3
NCOA4
NCOR1
NFE2L2
NFKBIE
NONO
NOTCH3
NSD2
NSD3
NT5C2
P2RY8
PAK1
PAK3
PARP1
PARP2
PARP3
PAX7
PDGFB
PDK1
PHF6
PIK3C2B
PIK3C2G
PIK3CB
PIK3CD
PIK3CG
PIK3R2
PLAG1
PLCG2
PML
POLD2
POLD3
POLD4
POLH
POLQ
PPM1D

TABLE A2. Gene List for the Subset of Whole Exome Panel Genes Sequenced at High Coverage and Read Depth (continued)

Genes
PPP2R2A
PPP6C
PREX2
PRF1
PRKACA
PRKCH
PRKCI
PRKN
PRSS1
PRSS8
PTCH2
PTK2B
PTPN22
PTPRD
PTPRO
PTPRT
QKI
RAD21
RAD51
RAD51B
RAD52
RAD54B
RAD54L
RANBP2
RARA
RASA1
RBBP8
RBM10
RCAN1
RECQL4
REL
RELA
RHEB
RHOA
RINT1
RIT1
RPA1
RPA2
RPA3
RPA4
RPL10
RPL5
RPTOR
RRAS2
SEM1
SERPINB3
SET
SGK1

TABLE A2. Gene List for the Subset of Whole Exome Panel Genes
Sequenced at High Coverage and Read Depth (continued)

Genes
SH2B3
SLIT2
SMAD3
SMARCA1
SMC3
SNCAIP
SOS1
SOX9
SPTA1
SS18
SSBP1
STAG2
STAT4
STAT6
TAF1
TAL1
TAL2
TBX3
TCF3
TEK
TERF2IP
TET2
TFE3
TFEB
TFG
TIPARP
TLX3
TNF
TOP3A
TOP3B
TRAF3
TRAF7
TSHZ3
TYK2
TYRO3
UBE2T
VEGFA
WAS
XPA
XPO1
XRCC1
XRCC2
XRCC3
ZBTB2
ZFHX3
ZNF703
ZRSR2

TABLE A3. Genomic Regions Sequenced for PMS2, MSH6, MSH2, and MLH1

Chromosome	Start	Stop	Gene
chr7	5,986,749	5,987,635	PMS2
chr7	5,989,790	5,989,970	PMS2
chr7	5,991,963	5,992,072	PMS2
chr7	5,995,524	5,995,648	PMS2
chr7	5,997,316	5,997,438	PMS2
chr7	5,999,098	5,999,290	PMS2
chr7	6,002,443	6,002,651	PMS2
chr7	6,003,680	6,003,807	PMS2
chr7	6,003,962	6,004,073	PMS2
chr7	6,005,882	6,006,046	PMS2
chr7	6,008,987	6,009,029	PMS2
chr2	47,783,224	47,783,503	MSH6
chr2	47,790,912	47,791,133	MSH6
chr2	47,795,879	47,796,073	MSH6
chr2	47,798,596	47,801,165	MSH6
chr2	47,803,405	47,803,695	MSH6
chr2	47,804,895	47,805,037	MSH6
chr2	47,805,603	47,805,717	MSH6
chr2	47,806,189	47,806,368	MSH6
chr2	47,806,437	47,806,661	MSH6
chr2	47,806,764	47,806,870	MSH6
chr2	47,403,182	47,403,412	MSH2
chr2	47,408,386	47,408,565	MSH2
chr2	47,410,079	47,410,382	MSH2
chr2	47,412,399	47,412,570	MSH2
chr2	47,414,254	47,414,428	MSH2
chr2	47,416,281	47,416,439	MSH2
chr2	47,429,727	47,429,951	MSH2
chr2	47,445,533	47,445,667	MSH2
chr2	47,463,016	47,463,164	MSH2
chr2	47,466,643	47,466,818	MSH2
chr2	47,470,950	47,471,072	MSH2
chr2	47,475,010	47,475,280	MSH2
chr2	47,476,352	47,476,581	MSH2
chr2	47,478,257	47,478,529	MSH2
chr2	47,480,681	47,480,881	MSH2
chr2	47,482,764	47,482,959	MSH2
chr3	36,993,521	36,993,673	MLH1
chr3	36,996,604	36,996,719	MLH1
chr3	37,000,940	37,001,063	MLH1
chr3	37,004,386	37,004,484	MLH1
chr3	37,006,976	37,007,073	MLH1
chr3	37,008,799	37,008,915	MLH1
chr3	37,011,805	37,011,872	MLH1
chr3	37,011,996	37,012,109	MLH1
chr3	37,014,417	37,014,554	MLH1
chr3	37,017,491	37,017,609	MLH1
chr3	37,020,295	37,020,473	MLH1

(continued in next column)

TABLE A3. Genomic Regions Sequenced for PMS2, MSH6, MSH2, and MLH1 (continued)

Chromosome	Start	Stop	Gene
chr3	37,025,622	37,026,017	MLH1
chr3	37,028,769	37,028,942	MLH1
chr3	37,040,171	37,040,304	MLH1
chr3	37,042,253	37,042,341	MLH1
chr3	37,047,504	37,047,693	MLH1
chr3	37,048,502	37,048,619	MLH1
chr3	37,048,889	37,049,027	MLH1
chr3	37,050,471	37,050,663	MLH1

TABLE A4. Variants Considered Pathogenic/Likely Pathogenic for *PMS2, MSH6, MSH2,* and *MLH1*

MLH1	MSH2	MSH6	PMS2
R659*|c.1975C>T	c.942+3A>T	F1088fs|c.3261dupC	D414fs|c.1239delA
E102K|c.304G>A	R524P|c.1571G>C	F1088fs|c.3261delC	S46I|c.137G>T
I19F|c.55A>T	A636P|c.1906G>C	F1088fs|c.3260_3261dupCC	R107W|c.319C>T
R226*|c.676C>T	D660fs|c.1977dupA	T1219I|c.3656C>T	P246fs|c.736_741delins11
K84E|c.250A>G	A230fs|c.687dupA	K1233fs|c.3699_3702delAGAA	E410*|c.1228G>T
Q516*|c.1546C>T	E357*|c.1069G>T	R240*|c.718C>T	c.-3_19del22
E605del|c.1814_1816delAAG	A309fs|c.924_925dupAG	E1322*|c.3964G>T	E172fs|c.516delA
G67R|c.199G>A	C333Y|c.998G>A	E744fs|c.2230dupG	Q205P|c.614A>C
Q409*|c.1225C>T	A913fs|c.2736delA	E847*|c.2539G>T	Q237*|c.709C>T
c.116+5G>A	E262*|c.784G>T	F1104fs|c.3312delT	M1?|c.3G>A
P640S|c.1918C>T	G751R|c.2251G>A	W372*|c.1116G>A	M1?|c.2T>C
Y157fs|c.469delT	Q314*|c.940C>T	E1234fs|c.3699dupA	R563*|c.1687C>T
W538*|c.1614G>A	Q793*|c.2377C>T	R379fs|c.1135_1139delAGAGA	Y149fs|c.444delC
c.546-1G>A	Q690*|c.2068C>T	R1242H|c.3725G>A	I611fs|c.1831dupA
c.677+1delG	E483*|c.1447G>T	E708*|c.2122G>T	E109fs|c.325delG
P648L|c.1943C>T	N311fs|c.928delC	R248fs|c.741dupA	c.251-1G>C
c.208-1G>A	Q337*|c.1009C>T	R298*|c.892C>T	R211*|c.631C>T
N551fs|c.1653delC	W117*|c.351G>A	R248*|c.742C>T	E253*|c.757G>T
R755fs|c.2263dupA	G47fs|c.140delG	K218fs|c.651dupT	c.24-1G>A
E71*|c.211G>T	Q288*|c.862C>T	Q698*|c.2092C>T	c.706-1G>A
R265C|c.793C>T	c.942+2T>C	C694fs|c.2079dupA	Y519fs|c.1555_1573del19
c.884+1G>T	T806fs|c.2415_2431del17	V1160F|c.3478G>T	F231fs|c.690_691delGT
c.545+1G>A	G587R|c.1759G>C	R33fs|c.97_101delinsA	R315*|c.943C>T
A681T|c.2041G>A	F88fs|c.264delT	E877*|c.2629G>T	
C494fs|c.1480delT	c.366+1G>T	Q177*|c.529C>T	
D74fs|c.221_237del17	Q409fs|c.1226_1227delAG	K606fs|c.1815_1816delTA	
c.1559-2A>T	S271fs|c.811_814delTCTG	Q939*|c.2815C>T	
c.885-1G>C	G753*|c.2257G>T	W628*|c.1884G>A	
T117M|c.350C>T	G25fs|c.72_85del14	D380fs|c.1134_1135delAA	
L555R|c.1664T>G	c.1277-2A>G	G599fs|c.1794dupA	
C77Y|c.230G>A	E698fs|c.2091dupT	T1284fs|c.3847_3850dupATTA	
G98R|c.292G>C	c.1760-1G>T	H1248_S1257del|c.3744_3773del30	
D41H|c.121G>C	Q252fs|c.754delC	Q572*|c.1714C>T	
E78_S83del|c.232_249del18	Q377*|c.1129C>T	V717fs|c.2150_2153delTCAG	
A21E|c.62C>A	G71*|c.211G>T	N184fs|c.552_555delTAAA	
T82A|c.244A>G	G126fs|c.377delG	E1187fs|c.3561_3571del11	
K196fs|c.588delA	P259fs|c.775_776delinsT	E1234*|c.3700G>T	
D450fs|c.1348delG	G751R|c.2251G>C	G237fs|c.710delG	
E23*|c.67G>T	L556W|c.1667T>G	K125fs|c.375delA	
T82P|c.244A>C	P349L|c.1046C>T	T1085fs|c.3252dupT	
D41V|c.122A>T	G674D|c.2021G>A	c.3646+1G>T	
D41G|c.122A>G	R680*|c.2038C>T	G1292fs|c.3874_3890del17	
V506A|c.1517T>C		Q593*|c.1777C>T	
c.380+1G>A		c.3439-1G>T	
K618del|c.1852_1854delAAG		E30*|c.88G>T	
E37K|c.109G>A		Y977fs|c.2930dupA	
E324*|c.970G>T		E796fs|c.2386delG	
A21V|c.62C>T		F1245fs|c.3729_3732dupATTA	
E297*|c.889G>T		S330*|c.989C>G	

TABLE A4. Variants Considered Pathogenic/Likely Pathogenic for *PMS2, MSH6, MSH2,* and *MLH1* (continued)

MLH1	MSH2	MSH6	PMS2
Q742*|c.2224C>T		Y214*|c.642C>A	
		T86fs|c.255delC	
		R379fs|c.1128_1132delAAAGA	
		W970*|c.2910G>A	
		Q835*|c.2503C>T	
		D1112fs|c.3332_3335dupATGA	
		C783fs|c.2348_2349delGT	
		W50*|c.149G>A	
		S536fs|c.1607delG	
		S702*|c.2105C>G	
		R1035*|c.3103C>T	
		S1141fs|c.3419dupA	
		E956fs|c.2865dupA	
		R1068*|c.3202C>T	
		Y1066*|c.3198T>A	
		M1267R|c.3800T>G	
		G1105fs|c.3313_3334del22	
		F432S|c.1295T>C	
		R1176fs|c.3525delT	
		A1320fs|c.3959_3962delCAAG	
		K1004*|c.3009_3010delinsCT	
		G1292fs|c.3860_3872dup13	
		c.3647-1G>A	
		K1319fs|c.3951_3955dupTAGAA	
		K1140fs|c.3416dupG	
		Q593fs|c.1776delA	
		A1293fs|c.3876delA	
		A1320fs|c.3957delA	
		S564*|c.1691C>G	
		Q1146*|c.3436C>T	
		E544*|c.1630G>T	
		R1334Q|c.4001G>A	
		E1193K|c.3577G>A	
		R1076C|c.3226C>T	
		R495*|c.1483C>T	
		V1192fs|c.3573dupT	
		Q776*|c.2326C>T	
		c.3173-1G>T	
		C1165fs|c.3491dupT	
		L447fs|c.1340_1341delTG	
		S154*|c.461C>A	
		V1164fs|c.3490dupG	
		E368*|c.1102G>T	
		G56fs|c.166_178del13	
		P1295fs|c.3878_3881dupCTTG	
		R300fs|c.896dupA	
		Q1314fs|c.3938_3941dupTTCA	
		K1000fs|c.2999delA	
		P362fs|c.1085delC	

(continued on following page)

TABLE A4. Variants Considered Pathogenic/Likely Pathogenic for *PMS2, MSH6, MSH2,* and *MLH1* (continued)

MLH1	MSH2	MSH6	PMS2
		W50*|c.150G>A	
		K246fs|c.738_741delAAAA	
		A1293fs|c.3876_3877insCCATA	
		K545fs|c.1634_1637delAAGA	
		S156*|c.467C>G	
		S677fs|c.2029dupA	
		N984fs|c.2950_2951delAA	
		T928fs|c.2781dupT	
		R1172fs|c.3516_3517delAG	
		c.3172+1G>A	
		R732*|c.2194C>T	
		Q419*|c.1255C>T	
		Q160*|c.478C>T	
		A48fs|c.141_142delinsC	